# Investigating Oscillation Loss in Computational Islets

REU Site: Interdisciplinary Program in High Performance Computing

Gemma Gearhart[1], Shuai Jiang[2], Thomas J. May[3], and Jane Pan[4],
Graduate RA: Samuel Khuvis[4], Faculty Mentor: Matthias K. Gobbert[4],
Clients: Bradford E. Peercy[4] and Arthur Sherman[5]

[1]Division of Science, Mathematics and Computing, Bard College at Simon's Rock
[2]Department of Mathematics, Cornell University
[3]Department of Mathematics, Virginia Polytechnic Institute and State University
[4]Department of Mathematics and Statistics, University of Maryland, Baltimore County
[5]Laboratory of Biological Modeling, National Institutes of Health

Technical Report HPCF–2013–14, `www.umbc.edu/hpcf` > Publications

**Abstract**

The study of pancreatic $\beta$-cells comprises a crucial part of the study of the group of diseases known as diabetes. These cells exist in groups known as islets of Langerhans and are responsible for storing and producing insulin. They exhibit electrical bursting behavior during insulin production that correlates with the rate at which insulin is secreted into the bloodstream. Coupling is a natural process within islets that enables the cells to communicate with one another and transfer various ions and electrical currents; coupling of both voltage and metabolites can occur. We model multicellular islets using an existing system of seven ordinary differential equations to model beta cell function. We first treat metabolic coupling as independent and look for combinations of coupling strengths, initial conditions, and parameter values that lead to metabolic oscillation loss, which has been observed in previous studies using a two-cell model. We find examples of each of these three features that can cause $\beta$-cells to exhibit oscillation loss at particular values. Next, we simulate cells with mutated $K_{ATP}$ channels that remain open indefinitely, which have been described in experimental studies but not yet modeled. Simulations run with these mutations reveal the existence of a bursting death threshold, described by the least percentage of cells in the islet that must be mutated for electrical bursts to completely disappear. We determine that this threshold is independent of coupling strengths, cell distribution, and possibly islet dimension; however, we also determined that this threshold is not independent of the glucose influx rate.

# 1 Introduction

Diabetes mellitus is a group of diseases in which the body either does not have the capabilities of producing insulin or is not capable of producing sufficient amounts of insulin to compensate for the glucose that enters the body. When blood sugar levels are increased by the consumption of glucose, a healthy human body would naturally produce adequate amounts of insulin to remove excess glucose that could potentially be harmful if maintained.

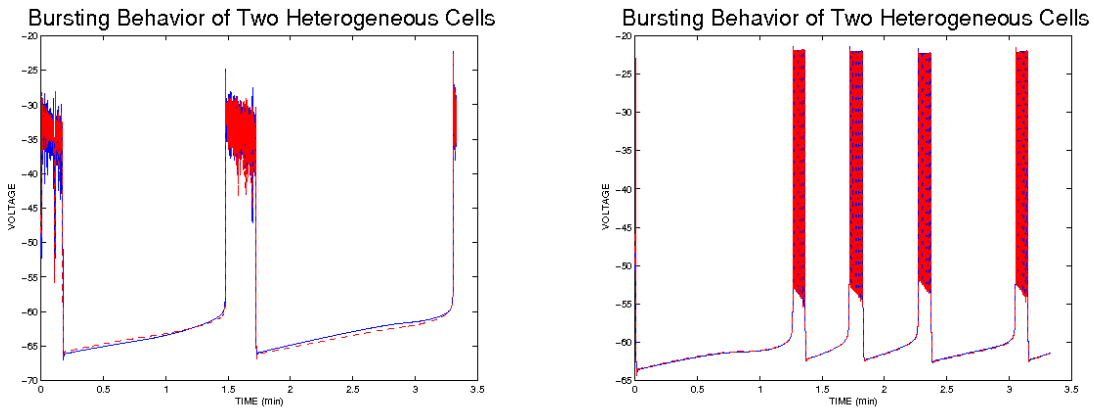


(a) (b)

Figure 1.1: (a) Oscillation behavior of two coupled $\beta$-cells with an electrical coupling value of 0.01 pS. (b) Oscillation behavior of the $\beta$-cells with an electrical coupling value of 0.1 pS.

The biological units that are responsible for the secretion of insulin are identified as $\beta$-cells [11], which are one of four hormone-producing cells located in the pancreas. Clusters of $\beta$-cells are known as islets of Langerhans, which depend on other islets within the pancreas to successfully carry out the production of insulin.

Previous studies have observed that $\beta$-cells undergo series of voltage oscillations during the course of insulin secretion. Once glucose enters the $\beta$-cell, the cell itself experiences an increase in ATP, which leads to the depolarization of the $\beta$-cell, allowing calcium to enter and insulin to be released into the bloodstream [8]. The frequency at which insulin is secreted correlates to the oscillating behavior of the cells.

Coupling is a natural process that occurs between cells within the islets of Langerhans. Gap junctions serve as pathways for the coupling that occurs between these cells, allowing for effective communication from cell to cell, including the transfer of ionic currents and calcium ions [1]. Previous findings have supported the notion that certain variations of coupling play a vital role in facilitating the production of insulin [11]. This can be seen primarily in the bursting patterns that the cells experience.

Figure 1.1 displays the oscillation behaviors of two heterogeneous $\beta$-cells when they are electrically coupled with one another. Both plots display continuous voltage alterations between rapid spiking behavior and stages of gradual increase. The rapid voltage oscillations denote the bursting action of the $\beta$-cells, signifying the release of insulin. The smooth lines following these rapid spiking phases represent the periods of rest before insulin is secreted again.

Cases in which the cells contain stronger electrical coupling strengths eventually become synchronized. Figure 1.1 contains the results that are obtained when the electrical coupling strength is sufficiently strong. It can be visually seen that the oscillations between the two cells are more harmonized, which suggests that the bursting behaviors between the two heterogeneous cells are similar. However,as coupling is strengthened the burst pattern can change. For example, the interburst interval is shortened in 0.1 pS coupling shown in

Figure 1.1(b) compared to 0.01pS coupling in Figure 1.1(a).

We are particularly interested in studying the factors that contribute to oscillation death. The term "death" is used to signify the loss in slow metabolic oscillations that the $\beta$-cells exhibit. We run simulations that implement various combinations of electrical and metabolic coupling by the metabolites fructose 1-6-biphosphate (FBP) and glucose 6-phosphate (G6P). Sherman [11] describes his simulations on a model containing two heterogeneous $\beta$-cells. Cases that were tested included coupling cells through a combination of electrical and FBP coupling whereas another case looked at the same coupling combination with the addition of G6P coupling [11]. The results that were obtained from these simulations suggest that oscillation deaths could be due to the addition of G6P coupling. We aim to extend Sherman's research by running simulations with larger islets of cells rather than just two cells. Since an islet of cells in the human body is generally around 1000 cells, it would be beneficial to run simulations using more realistic values and in order to confirm [the accuracy of] Sherman's proposed theory in the death of oscillations.

To approach this problem, we represent a computational islet using an $N \times N \times N$ cube. Our model uses a stiff system of seven ordinary differential equations per cell describing rates of change in voltage ($V$), fractions of open $K^+$ channels and concentrations of five chemical species. These equations can be found in Section 2.2.1. Using this model, there are various distributions that we can use to scrutinize the behaviors exhibited by the islet of cells [8].

Our research focuses primarily on the grouped and equal distribution models. Figure 1.2 provides a visual representation of the arrangement of the two cell types in each distribution. In the grouped structure, cells of the two heterogeneous types are arranged together and one cell type is coupled to the other type only along the middle layer of the islet. In the equally distributed structure, cells are arranged in an alternating pattern such that no cell is coupled to another cell of its own type. Using these particular distributions allows us to interpret two extremes of the possible models. More details on the implementation of the system of equations as well as an organized description on all of the different types of distributions can be found in sections 2.2.1 and 3.1 respectively.

Besides using these models to study the factors that bring oscillation deaths, we look at cases with distributions containing a certain proportion of mutated cells, in which the $K_{ATP}$ channels of the cells are always open. Similar to what we did for the first part of our research, we observe the bursting behaviors that result from the addition of these mutated cells. We also determine the specific proportion of mutated channels that serve as a threshold between oscillating patterns and oscillation deaths. Specific distributions of these mutated cells can be found in Section 3.3.

After running tests that focused on manipulating the coupling strengths and varying the proportions of cells with mutated $K_{ATP}$ channels, we were able to gain a clearer understanding on how these parameters play a role in the oscillating behavior of the cells. When determining the types of initial conditions that caused metabolic oscillations in $\beta$-cells, we found that certain combinations of coupling at specific ranges of coupling strengths cause gradual reduction in metabolic oscillations. Furthermore, we noticed that having greater than 74% mutated cells in the distribution causes metabolic oscillation death regardless of the conditions of the other parameters. Details on specific inputs and results we obtained

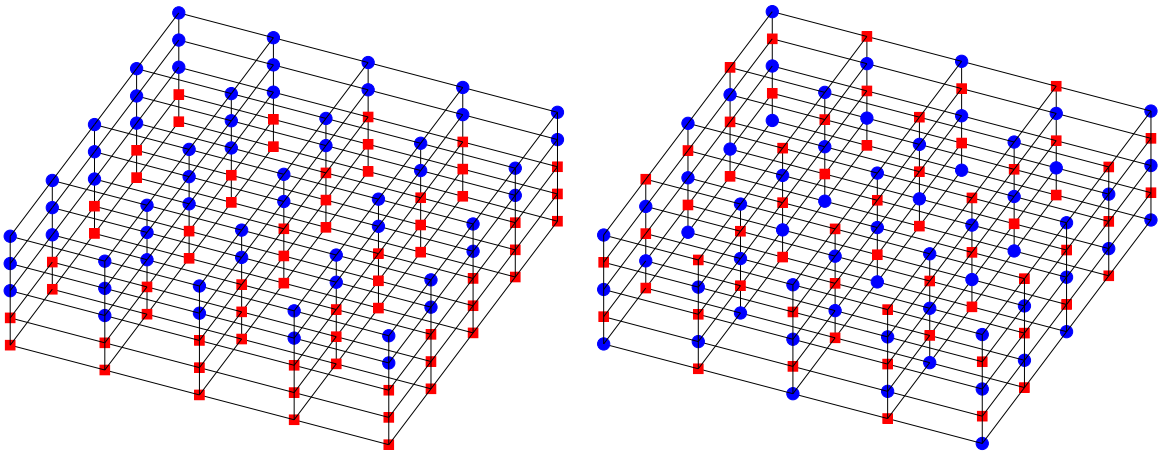

(a) (b)

Figure 1.2: The colors, red and blue, are used to represent the two different cell types that exist in the (a) grouped structure and (b) equally distributed structure.

can be found in Section 4. Final conclusions are made in Section 5.

# 2 Background

Insulin, produced by pancreatic $\beta$-cells, works by allowing muscles to absorb glucose and causing the liver and fat cells to process glucose. Type I diabetes is a type of diabetes in which the immune system attacks the $\beta$-cells; this results in uncontrolled glucose fluctuations and causes death if untreated. On the other hand, Type II diabetes is caused by increasing resistance to the effects of insulin, rather than the lack of $\beta$-cells directly. In the case that the $\beta$-cells are capable, they will increase production of insulin; in the case that they are not, a condition called hyperglycemia will occur, characterized by an excessive amount of glucose in blood plasma. Both cases will result in dramatic increases in heart disease risk, and in the later case, kidney damage, blindness, or peripheral neuropathy can occur. Currently, more than 25.8 million people in the United States suffer from diabetes [4], generating a large demand for relevant models of the pancreas and $\beta$-cells in particular.

The endocrine part of the pancreas contains clusters of cells called islet of Langerhans in which $\beta$-cells reside alongside three other types of cells. The models we examine only take $\beta$-cells into account since they are the only insulin-secreting cells. Section 2.1 provides a deeper discussion of physiology; secion 2.2 introduces the mathematical model we implement.

## 2.1 Physiology

Early studies have shown that $\beta$-cells exhibit oscillations of both voltage and calcium concentrations (denoted as [Ca]) [9]; these oscillations correlate with insulin secretion [5]. Oscillations are grouped in bursts of electrical activity. In addition, within the islet of Langerhans, $\beta$-cells are connected via intercellular connections called gap junctions; two cells that are connected through gap junctions are said to be coupled. Gap junctions allow small ions and products of metabolism, called metabolites, to flow between cells. It has been determined that these metabolites influence oscillations in $\beta$-cells and hence have an effect on insulin secretion [11].

Oscillations in voltage and metabolites, such as glucose 6-phosphate (G6P) and fructose 1-6-bisphosphate (FBP), occur when glucose enters $\beta$-cells through special protein channels in the cell membrane called glucose transporters (e.g., GluT1 or GluT2) via facilitated diffusion. This only occurs when the concentration of glucose outside the $\beta$-cell is high. The cell then metabolizes the glucose in the mitochondria and produces adenosine triphosphate (ATP). Increases in the concentration of ATP triggers depolarization of $\beta$-cell membranes by closing channels of ATP-sensitive ($K_{ATP}$) channels, which causes calcium to enter the cell. The subsequent influx of calcium and increase in [Ca] causes the release of vesicles containing insulin into the blood stream. Glucose levels are then decreased due to the release of insulin and the $\beta$-cell resets itself [7]. The reaction rate of glucokinase (called $R_{GK}$) reflects the level of glucose stimulation and does not change during the course of a simulation.

The $K_{ATP}$ channels that facilitate membrane depolarization are the main regulator of electrical activity in the islet, and glucose-stimulated insulin secretion relies on the sensitivity of these channels to ATP-inhibition. Mutations that render $K_{ATP}$ channels insensitive to ATP-inhibition suppress glucose-stimulated insulin secretion and alter voltage levels in the islet. Mutations of these channels can occur such that they remain either open or closed.

Since $K_{ATP}$ and [Ca] both contain a charge, the previously mentioned response to glucose will result in changes in voltage. Voltage tends to burst during the process of releasing insulin, with differing rates and variability among cells. Within the islet of Langerhans, the distribution of cells of differing voltage bursts is unknown. We use the distributions described in [8] to address this. These distributions are described in Section 3.1.

Multiple mathematical models of varying complexities have been developed to describe the dynamics between [Ca], electrical activity, and various metabolites. We utilize one of these models in our analysis.

## 2.2 Numerical Model

Our individual $\beta$-cell model uses a system of seven coupled ordinary differential equations (ODEs); a brief history of the development of the model is located in [8]. We view the islet as a cube of side-length $N$; there are $N \times N \times N$ total cells in our simulations.

### 2.2.1 Seven Variable Model Equations

We simulate $\beta$-cells using a model with glycolytic dynamics initially developed by Smolen [10] and combined with electrical dynamics by Bertram et al. [3] and studied in by Tsaneva-Atanasova et al. [11]. The model's dependent variables are voltage $V$, fraction of open potassium channels $n$, and other chemical concentrations including cyctosolic calcium $Ca$, endoplasmic reticulum calcium $Ca_{er}$, adenosine diphsophate ADP, adenosine triphosphate ATP, and metabolites glucose-6-phosphate G6P and fructose bisphophate FBP. The equations are

$$\frac{dV}{dt} = -\frac{I_{\mathrm{K}} + I_{\mathrm{Ca}} + I_{\mathrm{K(Ca)}} + I_{\mathrm{K(ATP)}}}{C_m}, \tag{2.1}$$

$$\frac{dn}{dt} = \frac{n_\infty - n}{\tau_n}, \tag{2.2}$$

$$\frac{d[\mathrm{Ca}]}{dt} = f_{\mathrm{cyt}}(J_{\mathrm{mem}} + J_{\mathrm{er}}), \tag{2.3}$$

$$\frac{d[\mathrm{Ca_{er}}]}{dt} = -\sigma_V f_{\mathrm{er}} J_{\mathrm{er}}, \tag{2.4}$$

$$\frac{d[\mathrm{ADP}]}{dt} = \frac{[\mathrm{ATP}] - [\mathrm{ADP}] \exp\left\{(r+\gamma)\left(1 - \frac{[\mathrm{Ca}]}{r_1}\right)\right\}}{\tau_a}, \tag{2.5}$$

$$\frac{d[\mathrm{G6P}]}{dt} = k(R_{\mathrm{GK}} - R_{\mathrm{PFK}}), \tag{2.6}$$

$$\frac{d[\mathrm{FBP}]}{dt} = k(R_{\mathrm{PFK}} - 0.5R_{\mathrm{GPDH}}), \tag{2.7}$$

where [XX] denotes the concentration of XX in the cytosol for Ca, ADP, G6P, FBP, and ERSurCaer. Additional definitions are

$$\begin{aligned}
I_{\mathrm{K}} &= \overline{g}_K n(V - V_{\mathrm{K}}),\\
I_{\mathrm{Ca}} &= \overline{g}_{\mathrm{Ca}} m_\infty(V)(V - V_{\mathrm{Ca}}),\\
I_{\mathrm{K(Ca)}} &= g_{\mathrm{K(Ca)}}(V - V_{\mathrm{K}}),\\
g_{\mathrm{K(Ca)}}([\mathrm{Ca}]) &= \frac{\overline{g}_{\mathrm{K(Ca)}}([\mathrm{Ca}])}{1 + \left(\frac{K_d}{[\mathrm{Ca}]}\right)^2},\\
I_{\mathrm{K(ATP)}} &= g_{\mathrm{KATP}}(V - V_{\mathrm{K}}),\\
g_{\mathrm{KATP}} &= \overline{g}_{\mathrm{K,ATP}} o_\infty([\mathrm{ADP}]),\\
m_\infty(V) &= \frac{1}{1 + \exp\left[-\frac{20+V}{12}\right]},\\
J_{\mathrm{er}} &= 0.0002([\mathrm{Ca_{er}}] - [\mathrm{Ca}]) - 0.4[\mathrm{Ca}],\\
J_{\mathrm{mem}} &= (4.5 \times 10^{-6}) I_{\mathrm{Ca}} - 0.2[\mathrm{Ca}],
\end{aligned}$$

where

$$o_\infty([\text{ADP}]) = \frac{0.08(1 + 2\frac{0.165[\text{ADP}]}{17}) + 0.89(\frac{0.165[\text{ADP}]}{17})^2}{(1 + \frac{0.165[\text{ADP}]}{17})^2 * (1 + \frac{0.135[\text{ADP}])}{26} + 0.05[\text{ATP}])}, \tag{2.8}$$

with constants: $C_m = 5300$ fF, $V_{\text{K}} = -75$ mV, $g_{\text{K}} = 2700$ pS, $\tau_n = 20$ ms, $g_{\text{Ca}} = 1000$ pS, $V_{\text{Ca}} = 25$ mV. The forms for consumption of G6P due to phosphofructose kinase $R_{\text{PFK}}$ and dehydrogenase consumption of FBP $R_{\text{GPDH}}$ can be found in [3]. Note that $R_{\text{GK}}$, $\overline{g}_{\text{KCA}}$, and $\overline{g}_{\text{K,ATP}}$ are parameters relating to bursting rates of electrical potential (voltage).

In order to couple the cells together, we define a matrix $G$ that contains the coupling strengths between each pair of cells. The matrix $G$ will be defined such that the coupling is diffusive ($\alpha(V_i - V_j)$ where $\alpha$ is the coupling strength, $V_i$ is the neighboring cell and $V_j$ is the current cell). Thus the differential equation can be written as

$$\frac{dy}{dt} = f(t, y) + Gy, \tag{2.9}$$

where $y = (V, n, [\text{Ca}], [\text{Ca}_{\text{er}}], [\text{ADP}], [\text{G6P}], [\text{FBP}])^T$ is a vector of length $7N^3$ (i.e., $V = [V_1, \ldots, V_{N^3}]^T$, etc.) and $f(t, y)$ is the right hand side of equations (2.1) - (2.7).

Using a similar model, the authors of [11] were able to demonstrate that oscillations in FBP and G6P concentrations will stop if certain parameters of two heterogeneous cell types are appropriate. We aim to be able to demonstrate that such "oscillation death" also occurs in multicellular computational islets.

# 3 Methodology

We now move to modifying the existing seven variable model for our study.

## 3.1 Simulating Metabolic Coupling

We start by extending an existing model [11] of the $\beta$-cell, which can handle electrical coupling already, to be able to handle G6P and FBP coupling. To implement these additions, our simulations use three matrices $C_V$, $C_{G6P}$, and $C_{FBP}$, where the $(a, b)$ entry of each matrix contains the coupling strength between the $a$th cell and the $b$th cell, $g_V$, $g_{G6P}$, and $g_{FBP}$, respectively. As in [8], $a$ and $b$ are indexed with $i + jN + kN^2$ being the one-dimensional index of the $(i, j, k)$-th cell. We now use these three matrices to define the matrix $G$ in (2.9) by

$$G = \begin{pmatrix} C_V & 0 & \cdots & 0 & 0 & 0 \\ 0 & 0 & \cdots & 0 & 0 & 0 \\ \vdots & \vdots & \ddots & \vdots & \vdots & \vdots \\ 0 & 0 & \cdots & 0 & 0 & 0 \\ 0 & 0 & \cdots & 0 & C_{G6P} & 0 \\ 0 & 0 & \cdots & 0 & 0 & C_{FBP} \end{pmatrix}.$$

The matrix is a $7 \times 7$ block matrix with blocks of size $N^3 \times N^3$. This formulation of $G$ allows (2.9) to simulate voltage, G6P, and FBP coupling while having no other coupling.

Since the distribution of heterogeneous cell types within the islet is unknown, we simulate the metabolically coupled islet with several different arrangements. Following the work of [8] on arrangements of two cell types, we use the arrangements of

1. *Grouped Structure*: The islet is split into two equally sized blocks of $\frac{N^3}{2}$ slow cells and $\frac{N^3}{2}$ fast cells.

2. *Equally Distributed Structure*: The islet is split so every neighbor of a slow cell is fast and ever neighbor of a fast cell is slow.

Since the feedback from the electrical subsystem onto the glycolytic subsystem is weak, we can effectively isolate the glycolytic sybsystem to locate a critical transition in parameters. In order to investigate the parameter space of where oscillation death, we vary the following parameter space in a $5 \times 5 \times 5$ islet:

1. **Coupling strength**: Vary the metabolic coupling strength of G6P and FBP across a range while holding initial conditions and other parameters the same.

2. **Initial Values of Metabolites**: Look through the four-dimensional parameter space of initial values in G6P and FBP for two heterogeneous cell types while holding other parameters the same.

3. $\mathbf{R}_{\mathrm{GK}}$ values: Change the $R_{\mathrm{GK}}$ values for two types of cells with different initial values.

## 3.2 Detecting Oscillations

We also implement a function which automatically determines if oscillation occurs in FBP concentrations in a cell, due to the large number of studies we run to obtain our results. This function gives time for the dynamics in the cell to stabilize and then uses a discrete derivative to examine if the absolute value of the estimated rate of change is above a certain threshold. If it is not, we classify the study to be non-oscillating and determine whether or not the difference is within a threshold limit of synchronous oscillation death (see Section 4.1.1).

While this algorithm catches most cases of oscillation death, there are cases, especially near the transition around oscillation dynamics, where this algorithm fails from large rest periods and lack of computational time. For example, Figure 3.1 demonstrates an example where a potential error could occur. If the simulation had only captured 10 minutes, the late oscillation would not have been detected. Formulating a method of detecting whether no oscillation will occur with greater accuracy can be the subject of a future study.

## 3.3 Simulating Mutations

In [2], Benninger experimentally studied the effects of mutated $\mathrm{K_{ATP}}$ channels on calcium oscillations in islets of $\beta$-cells in mice. We extend the seven variable model so that it can

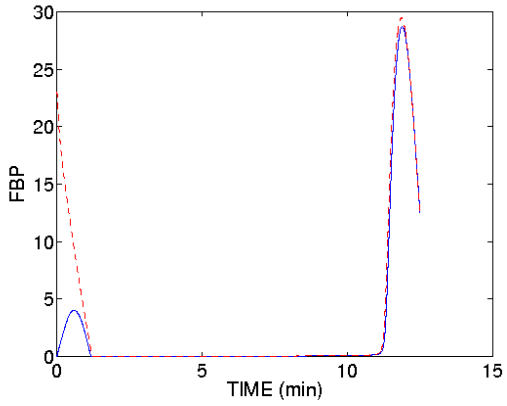


Figure 3.1: FBP in cell with $R_{GK} = 0.05$ $s^{-1}$ and $R_{GK} = 0.06$ $s^{-1}$.

handle cases in which a specified portion of cells in the islet have mutated $K_{ATP}$ channels that remain fully open or fully closed (see Section 2.1). Although our code is capable of simulating both mutation types, we only investigate the open mutation case; closed mutations are a possible direction for further study.

From [11], we know that $o_\infty([ADP])$ from (2.8) controls the open and closed behavior of $K_{ATP}$ channels; however, this number is not a fractional amount of open channels. In order to determine appropriate values for $o_\infty$ in mutated cells, we numerically solved the ODEs (2.1) - (2.7) under different coupling conditions and distributions and observed the values of $o_\infty$ during the run. Based on our observations, we set $o_\infty$ to 0.0075 for the open mutation as the largest observed values for $o_\infty$.

Given these observations, we redefine (2.8) to

$$o_\infty([ADP]) = \begin{cases} 0.0075 & : \text{Open Mutation} \\ \alpha([ADP]) & : \text{Normal Cell} \end{cases}, \tag{3.1}$$

where

$$\alpha([ADP]) = \frac{0.08(1 + 2\frac{0.165[\text{ADP}]}{17}) + 0.89(\frac{0.165[\text{ADP}]}{17})^2}{(1 + \frac{0.165[\text{ADP}]}{17})^2 * (1 + \frac{0.135[\text{ADP}])}{26} + 0.05[\text{ATP}])}.$$

For our investigations of islets with cells with open mutations, we are interested in two distributions with $m \leq N^3$ mutated cells and $N^3 - m$ non-mutated cells:

1. **Mutated Grouped**: Set cells 1 to $m$ to be mutated cells and cells $m+1$ to $N^3$ to be non-mutated cells.

2. **Mutated Spread**: Set cell 1 to be mutated. Start by calculating the the difference between the indices of all the non-mutated cells with all the mutated cells and find the smallest difference for each non-mutated cell. For the set of smallest differences, find the maximum value and set the cell whose difference is that maximum value to be the new mutated cell. Repeat until the number of mutated cells is $m$.

For the case of open mutations, the *burst death threshold* is the number of mutated cells in the islet required for no voltage bursts to be observed in the first 10 minutes of the simulation. The main focus of our mutation studies is to see how this threshold value is effected by different electrical and metabolic coupling, cell distributions, and $R_{\text{GK}}$ values. The different studies we run for the $5 \times 5 \times 5$ islet are as follows:

1. **Electrical Coupling Study**: This study varies electrical coupling strength from 25 pS to 600 pS incrementing by 25 pS while holding G6P and FBP coupling constant at 0.0 $\text{ms}^{-1}$ and $R_{\text{GK}}$ at 0.2 $\text{s}^{-1}$ for both types of distributions.

2. **FBP Coupling Study**: This study varies FBP coupling strength from 0 $\text{ms}^{-1}$ to 0.1 $\text{ms}^{-1}$ incrementing by 0.005 $\text{ms}^{-1}$ while holding G6P coupling constant at 0.0 $\text{ms}^{-1}$, voltage coupling at 100 pS, and $R_{\text{GK}}$ at 0.2 $\text{s}^{-1}$ for both types of distributions.

3. **G6P Coupling Study**: This study varies G6P coupling strength from 0 $\text{ms}^{-1}$ to 0.1 $\text{ms}^{-1}$ in increments of 0.005 $\text{ms}^{-1}$ while holding FBP coupling at 0.01 $\text{ms}^{-1}$, voltage coupling at 100 pS, and $R_{\text{GK}}$ at 0.2 $\text{s}^{-1}$ for both distributions.

4. **$\mathbf{R_{GK}}$ Study**: This study varies $R_{\text{GK}}$ from 0 $\text{s}^{-1}$ to 0.6 $\text{s}^{-1}$ incrementing by 0.025 $\text{s}^{-1}$ while holding voltage coupling at 100 pS, FBP coupling at 0 $\text{ms}^{-1}$, and G6P coupling at 0 $\text{ms}^{-1}$ for both types of distributions.

We also run a sampling of these studies for the $3 \times 3 \times 3$ islet to see if and how varying islet size affects the threshold.

## 3.4 Numerical Method

Given the different reaction rates of the system of differential equations (2.1) - (2.7), we have to treat this system as a stiff system of differential equations. We use a memory-modified version of Matlab's ode15s with automatic differentiation developed in [6] to run our simulations. Matlab's standard implementation of ode15s uses a version of Numerical Differentiation Formulas (NDFk), which is the standard method for stiff systems of differential equations. In order to solve the system, NDFk requires a Jacobian to be supplied, which Matlab allows to be handled in multiple ways. We supply a sparse Jacobian derived analytically using automatic differentiation, computed via the ADiMAT software developed by C. H. Bischof, H. M. Bücker, B. Lang, A. Rasch, and A. Vehreschild from the Institute for Scientific Computing, RWTH Aachen University, Germany. This is the optimal choice for our studies because it has a significant speedup compared to most other methods, as observed in [8], as well as allowing us to make modifications to the model in our simulations without having to recompute the Jacobian by hand.

Matlab's standard ode15s has significant speed and memory issues in solving the seven variable model even when supplied with a Jacobian found using automatic differentiation. The memory-modified version developed in [6] reduces the amount of memory allocated for each iteration of the process and removes the feature of ode15s which stores the gradient vector for each iteration since it is not used in any of the post-processing for our model.

Efficiency tests in [8] show that there is a significant speedup when the combination of ADiMat and the memory-modified ode15s is used, which allows for more simulations.

In addition, usage of Matlab's Parallel Computing Toolbox allowed for significantly higher simulation throughput. The command `parfor` ran many of our simulations in parallel on 8 computing cores, effectively increasing efficiency by eight times.

### 3.5 Description of the Computing Environment

The computations for this study were performed using the Matlab programming language (`www.mathworks.com`) under the Linux operating system on the cluster tara, located in the UMBC High Performance Computing Facility (`www.umbc.edu/hpcf`). The distributed-memory cluster tara consists of 86 nodes, with each node containing two quad-core Intel Nehalem X5550 processors (2.66 GHz, 8 MB cache) and 24 GB memory, thus up to 8 parallel processes can be run simultaneously per node. All nodes and the 160 TB central storage are connected by an quad-data rate InfiniBand interconnect.

## 4 Results

Our modifications to previous studies allow for metabolic coupling by the two metabolites glucose 6-phosphate (G6P) and fructose 1-6-bisphosphate (FBP) and enable us to study the effects of metabolic and electrical coupling on the oscillation behaviors exhibited by pancreatic $\beta$-cells. Using the extended capabilities of our model, we simulate and describe effects of varying parameters in a multicellular islet and extend our study to simulate islets in which some cells have mutated $K_{ATP}$ channels. See sections 3.1 and 3.3 for further techniques used in the objectives of our studies.

### 4.1 Oscillation Death

At certain combinations of electrical and metabolic coupling strengths, slow metabolic oscillations have been found to reduce and disappear in simulations run with a two-cell model [11]. We extend the findings of previous studies and consider a multicellular islet to observe for which initial conditions and coupling strengths we lose metabolic oscillations. To remain consistent with the model supplied by the study, we extend some portions of our implementation to include Matlab translations of XPP files that produced figures in [11]. For additional consistency, we include heterogeneity of cells by allowing for the coupling of two types of cells with different initial conditions and $R_{GK}$ values. Our simulations accept values for electrical, G6P, and FBP coupling strengths as parameters.

Figure 4.1 displays three classes of metabolic behavior that we observe in using our two types of heterogeneous cells when we vary coupling strengths and initial conditions of FBP and G6P; these classes are asynchronous oscillation death, synchronous oscillation death, and oscillation. Numerics can be used to show that these three types of dynamics can be observed within the metabolic components even in a two-cell case. In Figure 4.2, coupling

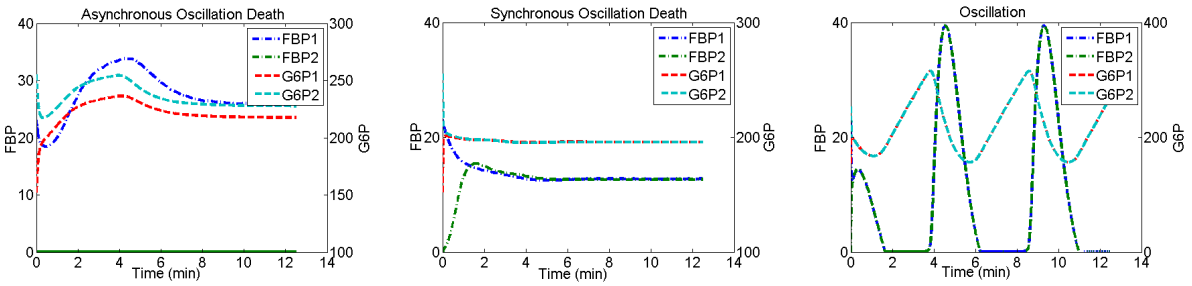


(a) (b) (c)

Figure 4.1: Classes of metabolic behavior: (a) asynchronous oscillation death with $g_V$ =75 pS, $g_{G6P}$ =0.01 ms$^{-1}$, and $g_{FBP}$ =0.001 ms$^{-1}$, (b) synchronous oscillation death with $g_V$ =75 pS, $g_{G6P}$ =0.1 ms$^{-1}$, and $g_{FBP}$ =0.001 ms$^{-1}$, (c) continued oscillation with $g_V$ =75 pS, $g_{G6P}$ =1 ms$^{-1}$, and $g_{FBP}$ =0.1 ms$^{-1}$.

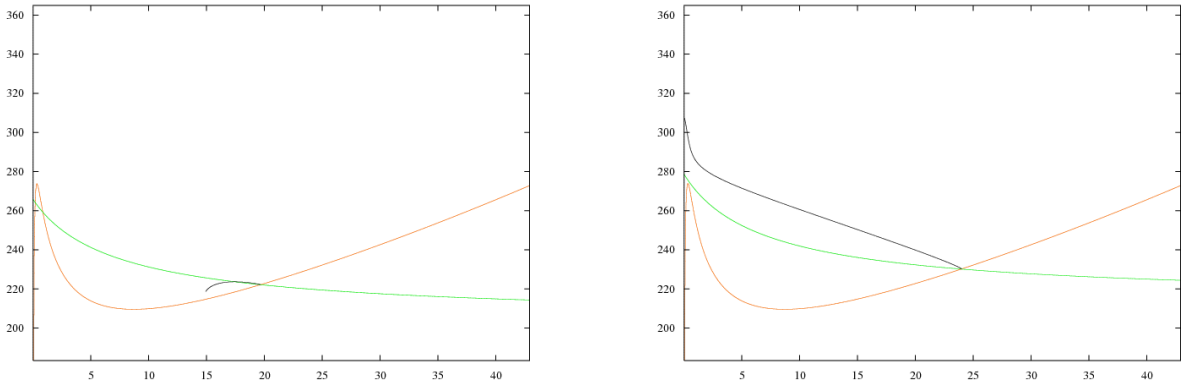

$R_{\mathrm{GK}} = .27$ $R_{\mathrm{GK}} = .4$

Figure 4.2: G6P and FBP nullclines of a two cell system for differing $R_{\mathrm{GK}}$.

is simulated by implementing a linear term and a vertical shift into the voltage, FBP and G6P equations. By adjusting the $R_{\mathrm{GK}}$ values from 0.27 to 0.4, we change the equilibria from a three equilibria system to a one equilibrium system, effectively displaying a pitchfork bifurcation. This suggests that altering $R_{\mathrm{GK}}$ values might have a significant impact on a model with a larger cell count, which we examine in Section 4.1.3. For a more detailed analysis of this bifurcation in a two-cell case, see [11].

### 4.1.1 Observing the Effects of Metabolic Coupling on Oscillations

Oscillation death in the 2-cell case was observed with electrical coupling of 75 pS and metabolic coupling of 0.001 ms$^{-1}$ for FBP and 0.01 ms$^{-1}$ for G6P. Manipulating our model such that only two cells are coupled to one another, we were able to reproduce this behavior with the same parameters. However, applying the same parameters to a multicellular islet

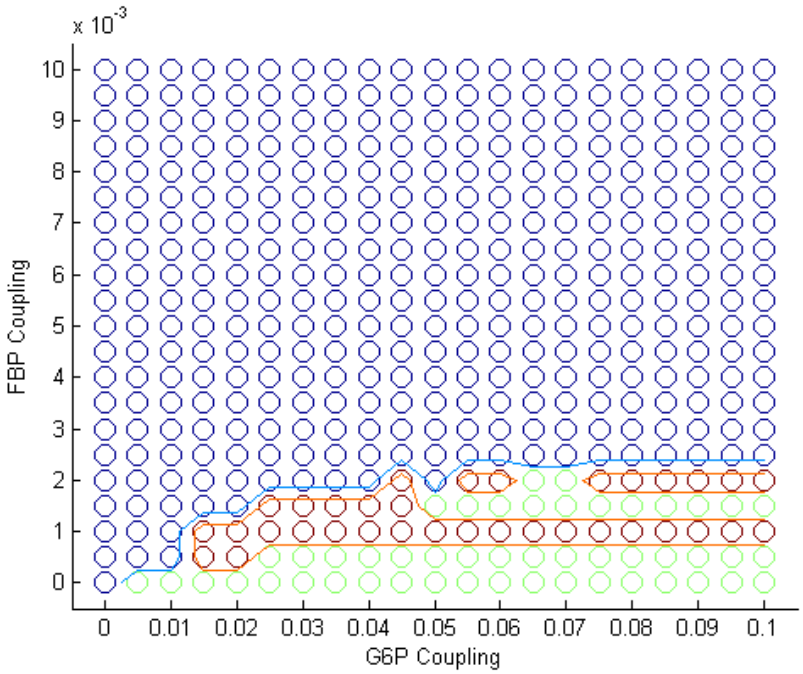


Figure 4.3: Scatter plot with contour lines separating regions of different oscillation behavior. Blue signifies continued oscillation, red signifies synchronous oscillation death, and green signifies asynchronous oscillation death.

of $5 \times 5 \times 5$ $\beta$-cells with the grouped and equal distributions, as detailed in 3.1, we find that oscillation death does not occur. In contrast, we observe metabolic oscillation death when all parameters are kept the same except for FBP coupling strength, which we decrease by a factor of 10. In following studies where we investigate the effect of altering initial conditions to test for oscillation loss, we use this updated combination of coupling strengths since we have confirmed that it can produce oscillation death in a multicellular islet.

While finding a single set of coupling strengths for which oscillation death occurs is desirable, as it confirms that these observations in the two-cell model also occur in the multicellular islet, the boundary in parameter space between continued oscillation and oscillation death is also of interest in our studies. By running a study in which we varied the G6P coupling strength from 0 $\text{ms}^{-1}$ to 0.1 $\text{ms}^{-1}$ in steps of 0.005 $\text{ms}^{-1}$ and the FBP coupling strength from 0 $\text{ms}^{-1}$ to 0.01 $\text{ms}^{-1}$ in steps of 0.0005 $\text{ms}^{-1}$, we produce Figure 4.3. We see that for the given initial conditions and electrical coupling strength, which are held constant, all three types of metabolic behavior occur as we vary the coupling strengths of the two metabolites.

### 4.1.2 Initial Conditions

We are interested in combinations of initial conditions and coupling strengths that result in bistable solutions, particularly in asynchronous oscillation death, shown in Figure 4.1(a). Due to the dynamics of the two metabolites, the initial values heavily influence which basin of

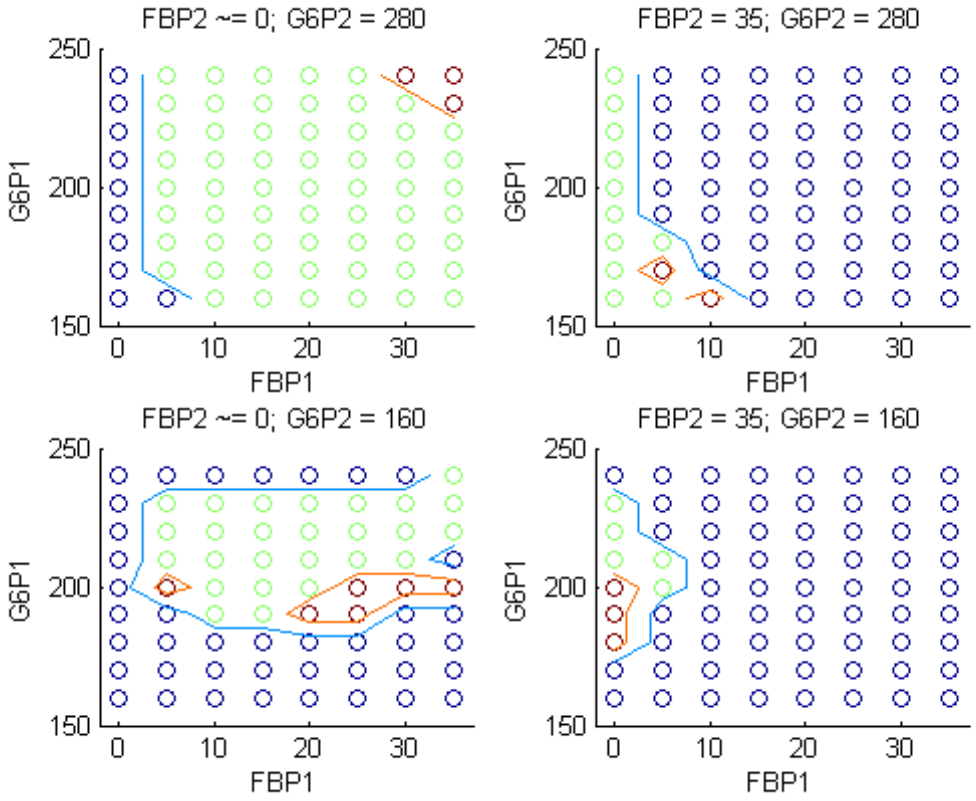


Figure 4.4: Coupling strengths kept constant at $g_V$ =75 pS, $g_{G6P}$ =0.01 ms$^{-1}$, and $g_{FBP}$ =0.001 ms$^{-1}$. Blue regions signify continued oscillation, green regions signify asynchronous oscillation death, and red regions signify synchronous oscillation death.

attraction the behavior will demonstrate. Figure 4.4 plots slices of the four dimensional space composed of varying the initial concentrations of FBP and G6P in two heterogeneous cell types. Plots such as Figure 4.4 with regions showing basins of attraction can be constructed for a chosen set of coupling strengths on a mesh of initial concentrations of G6P and FBP in the two types of cells, allowing us to predict the class of solution of our multicellular islet. Providing a perturbation sufficient to alter the concentrations of the two metabolites so that they lie in a different basin of attraction, we can switch between bistable solutions; this extends the previous result in coupled cells in [11] to the multicellular islet.

### 4.1.3 Varying $R_{\mathrm{GK}}$ Values

Many of our simulations use values of $R_{\mathrm{GK}}$ fixed at 0.2 s$^{-1}$ and 0.25 s$^{-1}$ for the two heterogeneous cell types. Preliminary runs which use coupling strengths and initial conditions as described in previous studies but set a single $R_{\mathrm{GK}}$ value shared by both cell types suggest that oscillation death can also occur as a result of altering this parameter. Plots from these preliminary runs with $R_{\mathrm{GK}}$ values of 0.35 s$^{-1}$ and 0.45 s$^{-1}$ in both cell types can be seen in

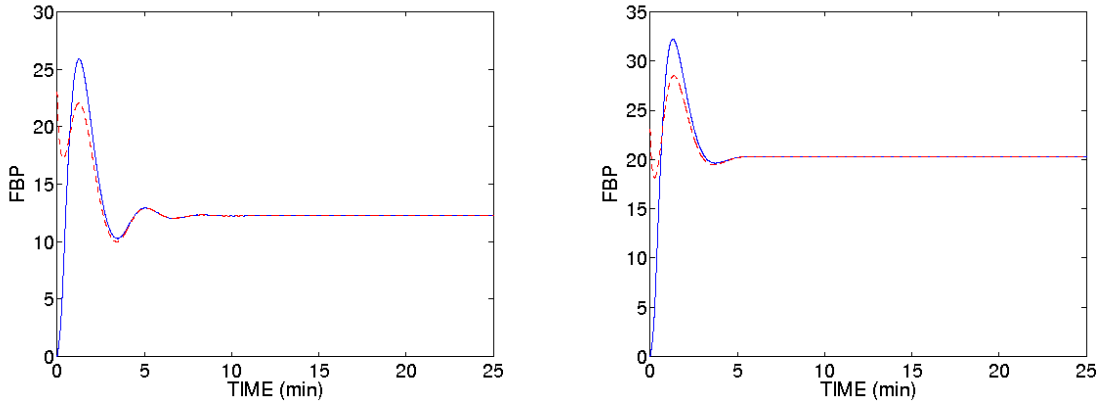


$R_{GK} = 0.35$ s$^{-1}$ $R_{GK} = 0.45$ s$^{-1}$

Figure 4.5: Parameter values and initial conditions are as described in 7(c) of [11], except $R_{GK}$ which is set to the values given, in both types of cells.

Figure 4.5. Runs with both values display synchronous oscillation death in the islet.

Varying $R_{GK}$ and reintroducing heterogeneity of this parameter reveals that certain combinations of $R_{GK}$ values in the two cell types result in asynchronous or synchronous oscillation death. As the rest periods between oscillations get longer and longer, we encounter a problem with the oscillation detection that we use (see Section 3.2) such that we were not able to conclusively determine which long-term behavior the metabolites were exhibiting. This problem is magnified greatly for small $R_{GK}$ values – for an example, see Figure 3.1. Thus, though we can observe oscillation death in particular cases while varying values of $R_{GK}$, accurate contour plots summarizing our tests could not be created until a better oscillation detection method is developed.

## 4.2 Observing the Effects of Open $K_{ATP}$ Channel Mutations

Our model considers two types of $K_{ATP}$ channel mutations: always open, which has harmful effects, and always closed, which has protective effects. We investigate only the case of open mutations but include simulation capabilities of both cases in our model. These mutations alter the sensitivity of $K_{ATP}$ channels to ATP-inhibition, which changes the value of the current $I_{K(ATP)}$ and, in consequence, the cell's voltage (see (2.1)). Based on this structure of influence within our model, we expect that the presence of mutated cells in the islet will affect voltage oscillations most severely. We expect the degree of influence to depend on the percentage of cells in the islet with channel mutations.

We conduct a detailed study of electrical oscillation behavior as open $K_{ATP}$ channel mutations are introduced into a $5 \times 5 \times 5$ computational islet with an $R_{GK}$ value of 0.2 s$^{-1}$ in both types of cells. As the number of mutated cells increases, the number of voltage bursts observed in cells in the islet gradually decreases. Voltage bursts continue to reduce until they eventually disappear when 93 of the 125 cells, or 74 percent, are mutated. For

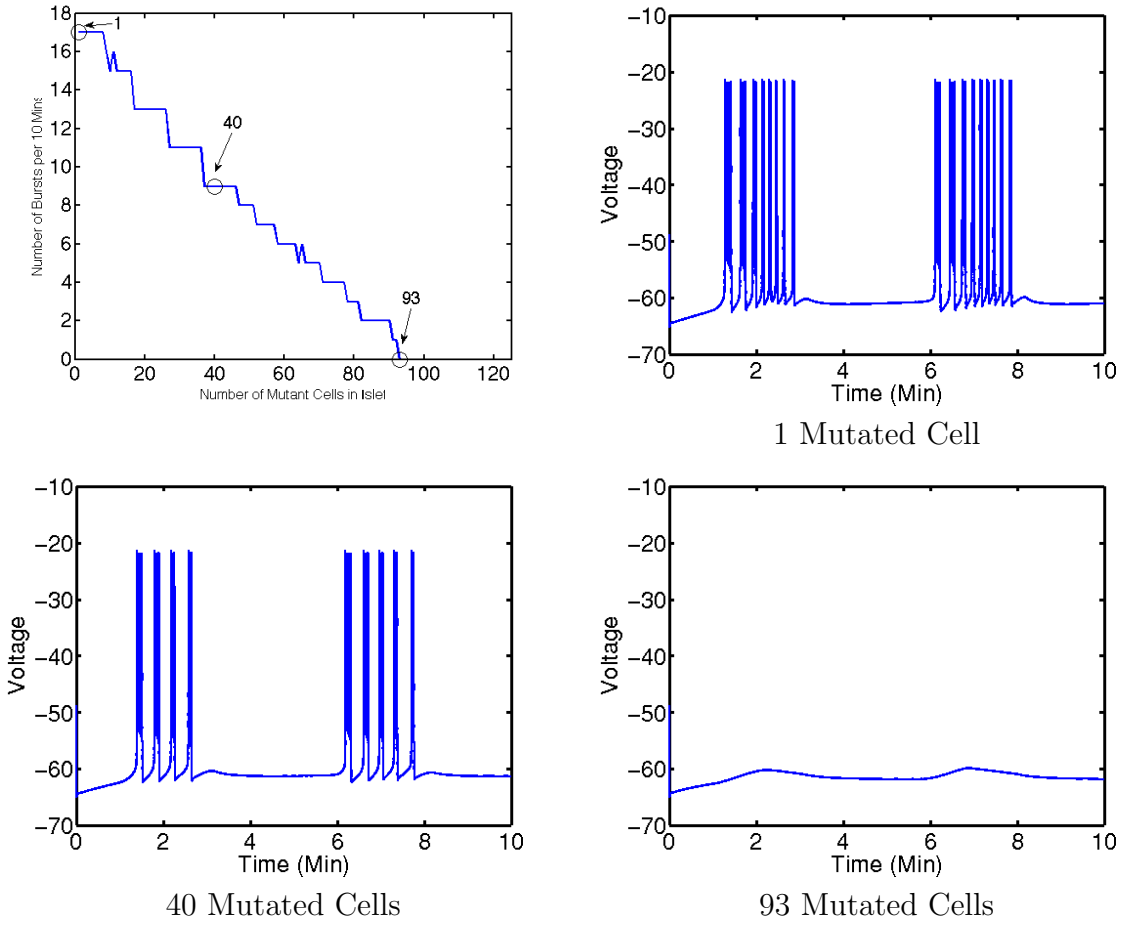


Figure 4.6: Voltage bursting as mutated cells are introduced into the $5 \times 5 \times 5$ islet. Coupling strengths kept constant at $g_V$ =75 pS, $g_{G6P}$ =0 $\text{ms}^{-1}$, and $g_{FBP}$ =0 $\text{ms}^{-1}$. $R_{\text{GK}}$ is 0.2 $\text{s}^{-1}$.

the parameters used in this run, we observe the same bursting death threshold of 74 percent mutated cells in a $3 \times 3 \times 3$ islet, suggesting that the threshold is independent of islet size.

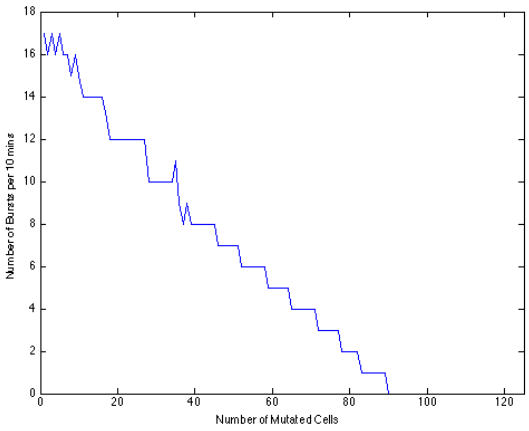


Figure 4.8: Voltage bursting as mutated cells are introduced into the $5 \times 5 \times 5$ islet. Coupling strengths kept constant at $g_V$ =100 pS, $g_{G6P}$ =0.035 ms$^{-1}$, and $g_{FBP}$ =0.01 ms$^{-1}$. $R_{\mathrm{GK}}$ is 0.2 s$^{-1}$.

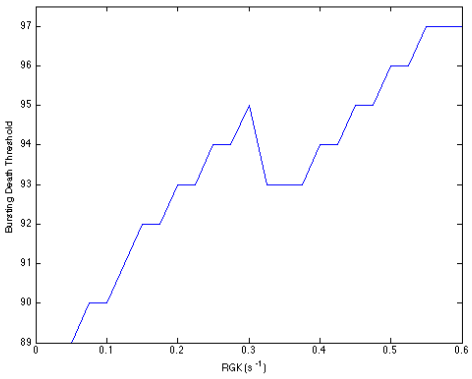


| $R_{\mathrm{GK}}$ | Threshold | $R_{\mathrm{GK}}$ | Threshold |
|---|---|---|---|
| 0.050 | 89 | 0.350 | 93 |
| 0.075 | 90 | 0.375 | 93 |
| 0.100 | 90 | 0.400 | 94 |
| 0.125 | 91 | 0.425 | 94 |
| 0.150 | 92 | 0.450 | 95 |
| 0.175 | 92 | 0.475 | 95 |
| 0.200 | 93 | 0.500 | 96 |
| 0.225 | 93 | 0.525 | 96 |
| 0.250 | 94 | 0.550 | 97 |
| 0.275 | 94 | 0.575 | 97 |
| 0.300 | 95 | 0.600 | 97 |
| 0.325 | 93 | | |

Figure 4.7: Bursting death threshold vs. $R_{\mathrm{GK}}$.

Figure 4.6 shows the gradual loss of electrical bursting as the percentage of mutated cells in the islet increases. The behavior displayed corresponds to an islet coupled electrically but not metabolically; however, the behavior exhibited by islets with additional coupling parameters is analogous. Figure 4.8 gives the number of electrical bursts over 10 minutes vs. the number of mutated cells in a $5 \times 5 \times 5$ islet coupled metabolically as well as electrically. Compare this to the top left plot in Figure 4.6; we see that the threshold is the same in both computational islets.

We conduct a study of the effect of $R_{\mathrm{GK}}$ values on oscillation death threshold in the islet with open channel mutations by varying the value of $R_{\mathrm{GK}}$ and documenting the number of mutated cells for which electrical oscillations disappear. In this study, we hold coupling constant at $g_V$ =100 pS, $g_{G6P}$ =0 ms$^{-1}$, and $g_{FBP}$ =0 ms$^{-1}$ and do not consider heterogeneity

Table 4.1: Runtimes in HH:MM:SS for 200,000 ms with the range of islet dimensions $N \times N \times N$ considered in our studies comparing the original ode15s and the memory-modified ode15s code.

| $N \times N \times N$ | Original ode15s | Memory-Modified ode15s |
|---|---|---|
| $3 \times 3 \times 3$ | 00:00:28 | 00:00:21 |
| $4 \times 4 \times 4$ | 00:01:38 | 00:00:33 |
| $5 \times 5 \times 5$ | 00:04:07 | 00:00:46 |
| $6 \times 6 \times 6$ | 00:10:02 | 00:01:14 |
| $7 \times 7 \times 7$ | 00:24:26 | 00:01:45 |
| $8 \times 8 \times 8$ | 00:32:52 | 00:02:47 |
| $9 \times 9 \times 9$ | 00:48:47 | 00:04:51 |
| $10 \times 10 \times 10$ | 01:11:58 | 00:07:48 |

in the values of $R_{\text{GK}}$ in the two cell types. Figure 4.7 and the accompanying table contain the bursting death thresholds for multiple $R_{\text{GK}}$ values in the $5 \times 5 \times 5$ islet.

We have seen above that the bursting death threshold may be independent of islet dimensions. We observe through repeated runs with mutated cells with varied parameters that the threshold depends on $R_{\text{GK}}$ values in the islet but is independent of electrical and metabolic coupling strengths as well as of mutated cell arrangement within the islet. This threshold exists in every computational islet we considered in which cells with open channel mutations were introduced and increased.

## 4.3 Numerical Study

Efficiency studies were performed in [8] to show that the numerical implementation we use is optimized. We compare the original ode15s method with the memory-modified version to justify its continued use when we introduce metabolic coupling capabilities and associated computations into the model. Table 4.1 gives the wall clock time in HH:MM:SS for a simulation with coupling strengths of $g_V$ =75 pS, $g_{G6P}$ =0.01 ms$^{-1}$, and $g_{FBP}$ =0.001 ms$^{-1}$ for 200,000 ms in the grouped distribution. ADiMat software is used in both tests.

The results in Table 4.1 show significant improvement in simulation runtime, particularly as islet dimension $N$ increases. Islets in the human body have approximately 1,000 $\beta$-cells, which makes the performance of simulations run at $N = 10$ significant for biological applications.

# 5 Conclusions

Through our studies, we gained a better understanding of the effects of coupling on the oscillation and bursting behaviors of pancreatic $\beta$-cells. Oscillation behaviors exhibited by $\beta$-cells in our multicellular islet are similar but not the same as those obtained from simulations

run with two $\beta$-cells. Manipulating coupling strengths, initial conditions, and $R_{\mathrm{GK}}$ parameters that corresponded to two heterogeneous cell types all led to metabolic oscillation death within the islet for particular values. Methods we developed can predict the class of solution of our multicellular islet – whether it displays continuous oscillation, asynchronous oscillation death, or synchronous oscillation death – when given a specific set of initial conditions and coupling strengths.

Based on the tests we ran, we believe there is a correlation between metabolic oscillation death and the metabolite parameter G6P. When coupled only through voltage and FBP, the $\beta$-cells in our islets did not experience metabolic oscillation death. However, when G6P coupling was introduced into our model, the islet exhibited oscillation loss for certain coupling strengths. Furthermore, increasing FBP coupling appeared to restore oscillations. These observations may have biological implications.

When we ran simulations on islets containing cells with open $\mathrm{K_{ATP}}$ channel mutations, there was a clear reduction in electrical bursts as higher proportions of mutated cells were implemented in our islet. Through simulating islets with large proportions of mutated cells, we were able to determine a bursting death threshold describing the least number of mutated cells necessary for electrical bursting to be lost. In the case of our $5 \times 5 \times 5$ islet model ran with one possible set of parameter values (Section 4.2), we found this threshold to be 93 of the 125, or 74%. This percentage, though independent of coupling strengths, mutated cell arrangement, and possibly islet dimension, is not independent of $R_{\mathrm{GK}}$ values.

In further investigations, it would be of interest to perform simulations involving islets containing cells with closed $\mathrm{K_{ATP}}$ channel mutations. Our model includes the structures necessary to perform these simulations, and numerical tests have shown us that they can be run by setting the function $o_\infty$ to have the constant value 0.007, which is its minimum (see Section 3.3 for the details of this function). However, we did not investigate the closed mutation case, due mainly to time constraints.

Further tests could also be conducted to try to identify the specific range of coupling strengths that result in each one of the metabolic behaviors we describe in Figure 4.1. Looking ahead, we hope that our studies will be beneficial to researchers in the biological fields who can run experimental versions of our simulations to confirm the accuracy of results we obtained through our studies.

# Acknowledgments

These results were obtained as part of the REU Site: Interdisciplinary Program in High Performance Computing (`www.umbc.edu/hpcreu`) in the Department of Mathematics and Statistics at the University of Maryland, Baltimore County (UMBC) in Summer 2013. This program is funded jointly by the National Science Foundation and the National Security Agency (NSF grant no. DMS–1156976), with additional support from UMBC, the Department of Mathematics and Statistics, the Center for Interdisciplinary Research and Consulting (CIRC), and the UMBC High Performance Computing Facility (HPCF). HPCF (`www.umbc.edu/hpcf`) is supported by the National Science Foundation through the MRI

program (grant nos. CNS–0821258 and CNS–1228778) and the SCREMS program (grant no. DMS–0821311), with additional substantial support from UMBC. Co-author Jane Pan was supported, in part, by the UMBC National Security Agency (NSA) Scholars Program though a contract with the NSA. Graduate RA Samuel Khuvis was supported during Summer 2013 by UMBC.

# References

[1] Richard K. P. Benninger, W. Steven Head, Min Zhang, Leslie S. Satin, and David W. Piston. Gap junctions and other mechanisms of cell–cell communication regulate basal insulin secretion in the pancreatic islet. *J. Physiol.*, 589(22):5453–5466, 2011.

[2] Richard K. P. Benninger, M. S. Remedi, W. S. Head, A. Ustione, D. W. Piston, and C. G. Nichols. Defects in beta cell $Ca^{2+}$ signalling, glucose metabolism and insulin secretion in a murine model of $K_{ATP}$ channel-induced neonatal diabetes mellitus. *Diabetologia*, 54(5):1087–1097, 2011.

[3] Richard Bertram, Leslie Satin, Min Zhang, Paul Smolen, and Arthur Sherman. Calcium and glycolysis mediate multiple bursting modes in pancreatic islets. *Biophys. J.*, 87(5):3074–3087, 2004.

[4] Centers for Disease Control and Prevention. National diabetes fact sheet: national estimates and general information on diabetes and prediabetes in the United States, 2011. `http://www.cdc.gov/diabetes/pubs/pdf/ndfs_2011.pdf`, accessed September 02, 2013.

[5] H.-F. Chou and E. Ipp. Pulsatile insulin secretion in isolated rat islets. *Diabetes*, 39:112–117, 1990.

[6] Sidafa Conde, Teresa Lebair, Christopher Raastad, Virginia Smith, Kyle Stern, David Trott, Matthias K. Gobbert, Bradford E. Peercy, and Arthur Sherman. Enabling physiologically representative simulations of pancreatic beta cells. Technical Report HPCF–2010–21, UMBC High Performance Computing Facility, University of Maryland, Baltimore County, 2010.

[7] Joel Keizer and Gerhard Magnus. ATP-sensitive potassium channel and bursting in the pancreatic beta cell. a theoretical study. *Biophys. J.*, 56(2):229–242, 1989.

[8] Samuel Khuvis, Matthias K. Gobbert, and Bradford E. Peercy. Time-stepping techniques to enable the simulation of bursting behavior in a physiologically realistic computational islet. Submitted (2013).

[9] R. M. Santos, L. M. Rosario, A. Nadal, J. Garcia-Sancho, B. Soria, and M. Valdeolmillos. Widespread synchronous [ca2+]i oscillations due to bursting electrical activity in single pancreatic islets. *Pflugers Arch.*, 418(4):417–422, 1991.

[10] Paul Smolen. A model for glycolytic oscillations based on skeletal muscle phosphofructokinase kinetics. *J. Theor. Biol.*, 174(2):137–148, 1995.

[11] Krasimira Tsaneva-Atanasova, Charles L Zimliki, Richard Bertram, and Arthur Sherman. Diffusion of calcium and metabolites in pancreatic islets: Killing oscillations with a pitchfork. *Biophys. J.*, 90(10):3434–3446, 2006.